CHAOTIC PHENOMENA IN AN AUTONOMOUS CIRCUIT WITH NONLINEAR INDUCTOR

Yoshifumi Nishio †, Naohiko Inaba ‡ and Shinsaku Mori †

† Department of Electrical Engineering, Keio University
3-14-1 Hiyoshi, Kohoku-ku, Yokohama, 223 Japan
‡ Department of Information Science, Utsunomiya University
2753 Ishii-machi, Utsunomiya, 321 Japan

ABSTRACT: In this article an analytic investigation of the chaotic phenomena in an autonomous circuit which contains a nonlinear inductor. The circuit dynamics are described by a three-dimensional piecewise-linear differential equation. In the case that the nonlinear inductor is assumed to have ideal saturation $\phi - i$ characteristic, the solution of the equation is constrained onto a two-dimensional plane piecewisely. Therefore, one-dimensional Poincaré map can be derived strictly and it is proved to be chaos in the sense of Li-Yorke. The justifiability of the idealization of the nonlinear inductor is verified theoretically and experimentally.

INTRODUCTION

Recently many chaos-generating autonomous circuits have been proposed and analyzed. Almost all of these circuits include nonlinear resistors. There are very few discussions about chaos-generating autonomous circuits which do not contain nonlinear resistors except for the model reported by Akiyama et al.[1]. They have analyzed an autonomous circuit with Josephson element. Though the equivalent circuit of the Josephson element is usually represented by a linear capacitor, a nonlinear resistor and a nonlinear inductor, they have verified that chaotic phenomena can be observed in the case that the equivalent circuit of the Josephson element does not contain the nonlinear resistor[1]. However, the $\phi - i$ characteristic of the nonlinear inductor in the equivalent circuit of the Josephson element is represented by $i = \sin\phi$ and the rigorous analysis seems to be difficult.

In the mean time, Saito and we have proposed the analyzing method using the idealization of the $v - i$ characteristics of diodes and have verified that it is effective to clarify the mechanism of chaos for some circuits[2]-[4]. In the case that this idealization is considered, three-dimensional systems are degenerated into two-dimensional systems piecewisely and the phenomena can be explained by using one-dimensional discrete map.

In this article an autonomous three-dimensional circuit with nonlinear inductor is analyzed. The circuit model is shown in Fig. 1(a) and it contains no nonlinear resistors. The $\phi - i$ characteristics of the nonlinear inductor is shown in Fig. 1(b) and the measured characteristics is shown in Fig. 1(c). Note that our nonlinear inductor has negative inductance in the center region and that it is saturable inductor which is quite different from the nonlinear inductor in the equivalent circuit of the Josephson element.

In order to analyze the chaotic phenomena observed from the circuit, we use a degeneration technique which means that the nonlinear inductor in the circuit is assumed to exhibit ideal saturation characteristic. In the case that this degeneration technique is used, the solution of the equation is constrained onto a two-dimensional plane piecewisely. Therefore, one-dimensional Poincaré map can be derived strictly and it can explain the phenomena very well. Especially the Poincaré map is proved to be chaos in the sense of Li-Yorke[5] with computer assistance.

The justifiability of the idealization of the nonlinear inductor is verified theoretically and experimentally.

The equation discussed in this article is a new type of constrained equations applied to chaos-generating circuits. The results of this article show that the analyzing method using the idealization of the characteristics of nonlinear elements is also effective for nonlinear inductors.

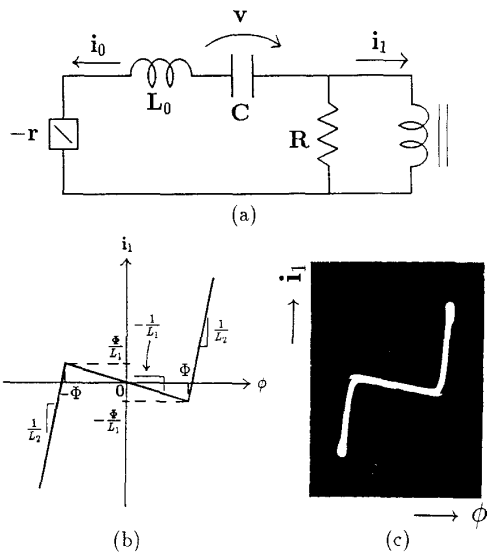

Fig. 1 Circuit model.

CIRCUIT MODEL

At first, we represent the $\phi - i$ characteristics of the nonlinear inductor by the following 3-segment piecewise-linear function as shown in Fig. 1(b).

$$i_1 = \frac{\phi}{L_2} - \left(\frac{1}{L_1} + \frac{1}{L_2}\right)\frac{|\phi + \Phi| - |\phi - \Phi|}{2} \tag{1}$$

Then the governing equation of the circuit is described by the following piecewise-linear three-dimensional differential equation.

$$\begin{aligned} \frac{d\phi}{dt} &= -Ri_0 - Ri_1 \\ C\frac{dv}{dt} &= i_0 \\ L_0\frac{di_0}{dt} &= (r - R)i_0 - v - Ri_1 \end{aligned} \tag{2}$$

CH2868-8/90/0000-0942$1.00 © 1990 IEEE

where ϕ, v and i_0 denote the magnetic flux in the nonlinear inductor, the voltage across C and the current through L_0, respectively. Note that the inductance L_2 in the saturate region of the nonlinear inductor is extremely small.

Via the rescaling,

$$\phi = \Phi x, \quad v = \frac{\Phi}{\sqrt{L_0 C}} y, \quad i_0 = \frac{\Phi}{L_0} z, \quad t = \sqrt{L_0 C}\tau,$$

$$\dot{} = \frac{d}{d\tau}, \quad \frac{L_0}{L_1} = \alpha, \quad \frac{L_0}{L_2} = \frac{1}{\varepsilon}, \quad r\sqrt{\frac{C}{L_0}} = a, \quad R\sqrt{\frac{C}{L_0}} = b, \tag{3}$$

the normalized equation is represented as follows.

$$\begin{aligned} \dot{x} &= -bf(x) \\ \dot{y} &= z \\ \dot{z} &= (a-b)z - y - bf(x) \end{aligned} \tag{4}$$

where

$$f(x) = \frac{x}{\varepsilon} - \left(\alpha + \frac{1}{\varepsilon}\right)\frac{|x+1| - |x-1|}{2}. \tag{5}$$

Define,

$$\begin{aligned} D^+ &: x > 1 \\ D^o &: |x| < 1 \\ D^- &: x < -1. \end{aligned} \tag{6}$$

Equation (4) is linear in the each region. Equilibrium in D^o is the origin O and equilibria in $D^\pm$ are represented as follows.

$$P^\pm : (x, y, z) = (\pm(1+\varepsilon\alpha), 0, 0) \tag{7}$$

Eigenequations are represented as follows.

$$m^3 - (a - b + \alpha b)m^2 + (1 + \alpha a b)m - \alpha b = 0 \qquad \text{in } D^o \tag{8}$$

$$m^3 - \left(a - b - \frac{b}{\varepsilon}\right)m^2 + \left(1 - \frac{ab}{\varepsilon}\right)m + \frac{b}{\varepsilon} = 0 \qquad \text{in } D^\pm \tag{9}$$

In the following discussions, we consider the case that Eq. (7) (Eq. (8)) has one real and a pair of complex conjugate eigenvalues λ_o, $\sigma_o \pm j\omega_o$ (λ_p, $\sigma_p \pm j\omega_p$).

Let $E_1^\pm$ and $E_2^\pm$ be the eigenspaces in $D^\pm$ corresponding to the real eigenvalue λ_p and the complex-conjugate eigenvalues $\sigma_p \pm j\omega_p$, respectively. Similarly, Let E_1^o and E_2^o be the eigenspaces in D^o corresponding to λ_o and $\sigma_o \pm j\omega_o$, respectively. The eigenspaces are given by the following equation.

$$E_1^\pm : \frac{x \pm (1+\varepsilon\alpha)}{-\lambda_p b} = \frac{y}{\lambda_p + \frac{b}{\varepsilon}} = \frac{z}{\lambda_p(\lambda_p + \frac{b}{\varepsilon})},$$

$$E_2^\pm : \frac{b}{\varepsilon}\{x \pm (1+\varepsilon\alpha)\} + (1 - \sigma_p^2 - \omega_p^2)y + (2\sigma_p - a + b)z = 0,$$

$$E_1^o : \frac{x}{-\lambda_o b} = \frac{y}{\lambda_o - \alpha b} = \frac{z}{\lambda_o(\lambda_o - \alpha b)},$$

$$E_2^o : \alpha b x + (\sigma_o^2 + \omega_o^2 - 1)y + (a - b - 2\sigma_o)z = 0. \tag{10}$$

Furthermore let $L_b^\pm$ be an intersection of $E_2^\pm$ and $x = \pm 1$. Then $L_b^\pm$ is represented as follows.

$$L_b^\pm : x = \pm 1, \quad (1 - \sigma_p^2 - \omega_p^2)y + (2\sigma_p - a + b)z = \pm\alpha b \tag{11}$$

Figure 2 shows the geometric structure of the vector field at $(\alpha, \varepsilon, a, b)$=(0.5, 0.1, 0.3, 1). At these parameter values, eigenvalues are caluculated as follows.

$$\begin{aligned} \lambda_p &= -10.97, \qquad \sigma_p \pm j\omega_p = 0.13 \pm j0.95, \\ \lambda_o &= 0.37, \qquad \sigma_o \pm j\omega_o = -0.28 \pm j1.13. \end{aligned} \tag{12}$$

Since ε is very small, λ_p is negative and large and $E_2^\pm$ is close by the boundary $x = \pm 1$. Therefore, it is considered that trajectories in $D^\pm$ oscillate around $P^\pm$ flatten onto $E_2^\pm$ rapidly and hit the boundary $x = \pm 1$ near $L_b^\pm$.

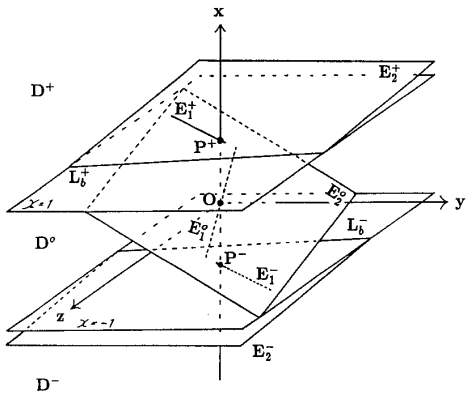

Fig. 2 Geometric structure of the vector field.

Figure 3 shows the projections of the chaotic attractor onto $x - y$ plane and $y - z$ plane. At these parameter values, asymmetric chaotic attractors coexist located symmetrically with respect to the origin. In this case, trajectories starting from D^+ do not enter D^-. Therefore, for the sake of the simplicity, we consider the case that the nonlinear inductor has asymmetric $\phi - i$ characteristic as shown in Fig. 4(a). The symmetric case is considered later.

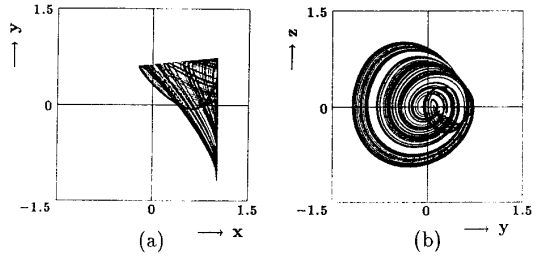

Fig. 3 An example of the chaotic attractor ($\alpha = 0.5$, $\beta = 0.02$, $a = 0.3$ and $b = 1$).
(a) Projection onto $x - y$ plane.
(b) Projection onto $y - z$ plane.

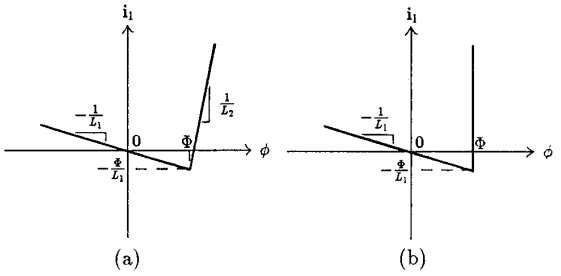

Fig. 4 The $\phi - i$ characteristics of the nonlinear inductor.

IDEAL MODEL

In order to investigate the phenomena generated in our model deeply, we use a degeneration technique. That is, the case where $L_2 \to 0$ as shown in Fig. 4(b) is considered. This idealization

represents that the saturation of the nonlinear inductor is ideal. In this case, the solution of Eq. (2) seems to be well explained by the following Ideal Model.

[Ideal Model]

1. when $\phi = \Phi$, (in D^+)

$$\begin{aligned} C\frac{dv}{dt} &= i_0 \\ L_0\frac{di_0}{dt} &= ri_0 - v. \end{aligned} \tag{13}$$

2. when $\phi < \Phi$, (in D^o)

$$\begin{aligned} \frac{d\phi}{dt} &= -Ri_0 + \frac{R}{L_1}\phi \\ C\frac{dv}{dt} &= i_0 \\ L_0\frac{di_0}{dt} &= (r-R)i_0 - v + \frac{R}{L_1}\phi. \end{aligned} \tag{14}$$

Note that i_1 in D^+ can be obtained by using the relation $d\phi/dt = 0$ in Eq. (2).

These equations in D^+ and D^o are connected by the following transitional conditions.

$D^+ \rightarrow D^o$: when i_1 decreases and reaches $-\Phi/L_1$.
$D^o \rightarrow D^+$: when ϕ increases and reaches Φ.

Via the rescaling (3), the normalized equation is represented as follows.

1. when $x = 1$, (in D^+)

$$\begin{aligned} \dot{y} &= z \\ \dot{z} &= -y + az. \end{aligned} \tag{15}$$

2. when $x < 1$, (in D^o)

$$\begin{aligned} \dot{x} &= -bz + \alpha bx \\ \dot{y} &= z \\ \dot{z} &= (a-b)z - y + \alpha bx. \end{aligned} \tag{16}$$

and the transitional conditions are follows.

$$D^+ \rightarrow D^o : z = \alpha, \qquad D^o \rightarrow D^+ : x = 1. \tag{17}$$

Though we omit the detailed proof due to space restrictions, we can verify the justifiability of the Ideal Model by proving the following.

$$\begin{aligned} &\lim_{\varepsilon \to 0} \lambda_p = -\infty \\ &\lim_{\varepsilon \to 0} E_2^+ = \{(x,y,z) | x = 1\} \\ &\lim_{\varepsilon \to 0} L_b^+ = \{(x,y,z) | z = \alpha\} \end{aligned} \tag{18}$$

These equations are proved by expanding the eigenvalues into the power series of ε and show that the vector field of Eq. (4) converges to that of the Ideal Model.

POINCARÉ MAP

Figure 5 shows the projection of the vector field onto $y - z$ plane. Define

$$L_m : x = 1, \quad y < 0, \quad z = 0. \tag{19}$$

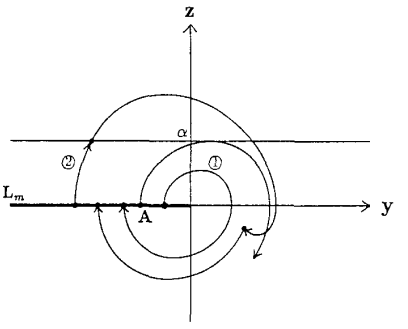

Fig. 5 Projection of the vector field onto $y - z$ plane.

Consider the solution having the initial condition on L_m, that is the solution starting from $(x, y, z) = (1, y_0, 0)$ $(y_0 < 0)$. Let A be the value of y at an initial point on L_m whose flow should be tangent to the transitional condition $z = \alpha$ from D^+ to D^o.

① When $y_0 > A$: The solution hits L_m again without reaching the boundary $z = \alpha$.
② When $y_0 < A$: The solution hits the boundary L_m and enters D^o. Then, it hits the plane $x = 1$ and enters D^+ again. And it returns back to L_m again.

Therefore, one-dimensional Poincaré map can be derived as follows.

$$F : L_m \rightarrow L_m, \quad y_0 \rightarrow F(y_0) \tag{20}$$

where y_0 is the y-coordinate of the initial condition on L_m and $F(y_0)$ is the y-coordinate of the point on L_m to which the solution leaving L_m returns back.

Usually, we have to solve implicit functions numerically in order to obtain the time when solutions hit boundaries. Hence, we can not represent Poincaré maps explicitly. However, in this case we can represent the Poincaré map explicitly by taking the amount of time the solution stays in D^o as the parameter.

Figure 6 shows an example of the Poincaré map. At these parameter values it satisfies the Li-Yorke's period three condition[5].

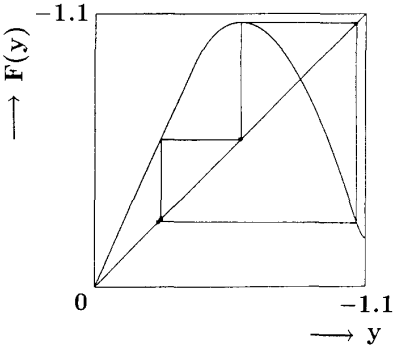

Fig. 6 An example of the Poincaré map F ($\alpha = 0.5$, $a = 0.25$ and $b = 1$).

Figure 7 shows the one-parameter bifurcation diagram of the Poincaré map F. Figure 8 shows the experimental and the associated simulated results.

Lastly, the symmetric case is considered. Figure 9 shows an example of the chaotic attractor in the symmetric case. In this case, the one-dimensional Poincaré map can be derived similarly. However, it has infinitely many extrema and its rigorous analysis seems to be difficult.

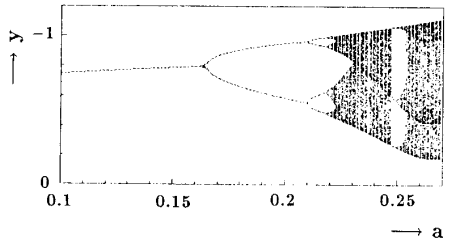

Fig. 7 One-parameter bifurcation diagrams of F.

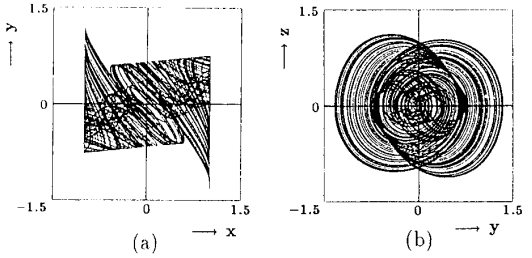

Fig. 9 An example of the chaotic attractor in the symmetric case ($\alpha = 0.5$, $a = 0.35$ and $b = 1$).

(a) Projection onto $x - y$ plane.

(b) Projection onto $y - z$ plane.

CONCLUSIONS

In this article we have analyzed an chaos-generating autonomous circuit which contains a nonlinear inductor. By considering the case that the nonlinear inductor is assumed to have ideal saturation $\phi - i$ characteristic, one-dimensional Poincaré map can be derived strictly and it is proved to be chaos in the sense of Li-Yorke with computer assistance. The justifiability of the idealization of the nonlinear inductor is verified theoretically and experimentally.

REFERENCES

[1] K. Akiyama, K. Araki and M. Morisue, "Non-Periodic Oscillation at Josephson Autonomous System," Technical Report on Nonlinear Problem of IEICE, vol. NLP-89-6, pp. 35-39, Sep. 1989.

[2] N. Inaba, T. Saito and S. Mori, "Chaotic Phenomena in a Circuit with a Negative Resistance and an Ideal Switch of Diodes," Trans. IEICE, vol. E-70, pp. 744-754, Aug. 1987.

[3] Y. Nishio, N. Inaba, S. Mori and T. Saito, "Rigorous Analyses of Windows in a Symmetric Circuit," Proc. ISCAS'89, pp. 2151-2154, 1989.

[4] Y. Nishio, N. Inaba and S. Mori, "Chaotic Phenomena in a Four-Dimensional Circuit with Two Ideal Diodes," Proc. ECCTD'89, pp. 157-161, 1989.

[5] T. Y. Li and J. A. Yorke, "Period Three Implies Chaos," Amer. Math. Monthly, vol. 82, pp. 985-992, 1975.

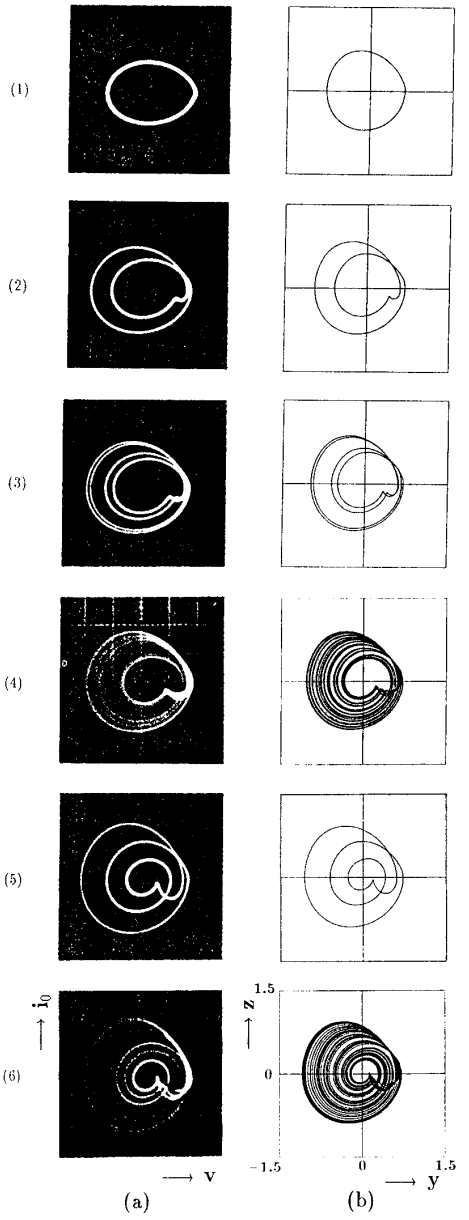

Fig. 8 Experimental and the associated simulated results ($\alpha = 0.5$ and $b = 1$).

(a) Experimental results.

(b) Simulated results.

(1) 1-period (a)$a = 0.1500$,(b)$a = 0.2323$.

(2) 2-period (a)$a = 0.2000$,(b)$a = 0.2760$.

(3) 4-period (a)$a = 0.2150$,(b)$a = 0.2855$.

(4) Chaos (a)$a = 0.2400$,(b)$a = 0.3094$.

(5) 3-periodic window (a)$a = 0.2475$,(b)$a = 0.3266$.

(6) Chaos in the sense of Li-Yorke (a)$a = 0.2600$,(b)$a = 0.3398$.